Biomass Conversion and Biorefinery
https://doi.org/10.1007/s13399-023-04597-9

ORIGINAL ARTICLE

Amino functionalized metal–organic framework as eco-friendly support for enhancing stability and reusability of horseradish peroxidase for phenol removal

Mustafa Zeyadi[1] · **Yaaser Q. Almulaiky**[2,3]

Received: 1 May 2023 / Revised: 4 July 2023 / Accepted: 6 July 2023

Abstract
Phenolic compounds are expected to be successfully removed from wastewater as pervasive environmental contaminants. For the removal of phenolic chemicals, enzymes such as horseradish peroxidase have shown to have a lot of promise. Horseradish peroxidase (HRP) was immobilized on amino functionalized metal organic frameworks (NH_2-MOF-Zr) utilizing covalent bonds. The microstructural and physicochemical properties were investigated using Fourier transform infrared (FT-IR), X-Ray diffraction (XRD) analysis, and scanning electron microscopy (SEM). The free HRP and NH_2-MOF-Zr@HRP were characterized by determining the activity profile as a function of kinetic behavior, pH, storage stability, effect of organic solvent, and temperature. The Km and Vmax for NH_2-MOF-Zr@HRP were estimated to be 34.7 mM, 0.811 U/mL for guaiacol and 12.58 mM, 0.930 U/mL for H_2O_2, respectively. The optimum pH values of the enzyme activity were found as 7 and 7–7.5 for the free HRP and NH_2-MOF-Zr@HRP, respectively. The optimum temperature profile of the free HRP and NH_2-MOF-Zr@HRP revealed as 40 °C and 50 °C, respectively. NH_2-MOF-Zr@HRP maintained 74% of its initial activity after 6 weeks of storage and 59% of its initial activity after ten consecutive cycles of the guaiacol oxidation. A substantial degree of the phenolic compounds was removed by HRP immobilized on the NH_2-MOF-Zr. About 87%, 53%, and 49% of 4-methoxyphenol (4-MEP), bisphenol A (BPA), and phenol were removed by NH_2-MOF-Zr@HRP during a 6-h reaction. The removal efficiency of phenol, BPA, and 4-MEP after five reuse cycles was 48%, 51%, and 62%, respectively.

Keywords Environmental · Immobilization · Horseradish peroxidase · Metal organic frameworks · Reusability

1 Introduction

Anthropogenic impacts on the biosphere have unavoidably increased due to a growing number of contaminants, such as various organic pollutants, synthetic dyes, and polycyclic aromatic hydrocarbons, making it challenging for humans to eliminate hazardous pollutants from many industries [1]. Phenolic compounds are essential components in the chemical industry. They are also regarded as pervasive environmental pollutants, though, as the wastewater that is discharged has only received partial treatment. One source of phenolic pollution is the widespread use of everyday items such phenoxy herbicides, petrochemicals, and wood preservatives [2]. For instance, bisphenol A (BPA), a substance found in many food and beverage packaging materials, is readily disposed of in home sewage when washed and sterilized repeatedly [3]. Furthermore, during long-term storage, BPA may diffuse into foods and beverages, which may cause estrogenic activity in humans [4]. In actuality, numerous phenolic substances are known to alter hormones. They have a high level of toxicity for humans and can accumulate in the body, even at low amounts. Due to their high substrate specificity, high activity under milder conditions, and biodegradable nature, various plant, and microbial oxidoreductases (Horseradish peroxidase) have recently attracted more attention for detoxifying and degrading a wide range of dyes either by precipitation or by opening the aromatic ring structure [5]. In addition to being used to identify hydrogen peroxide

✉ Yaaser Q. Almulaiky
yaseralmoliki@hotmail.com

[1] Department of Biochemistry, Faculty of Science, King Abdulaziz University, P. O. Box 80200, 21589 Jeddah, Saudi Arabia

[2] Department of Chemistry, College of Science and Arts at Khulis, University of Jeddah, Jeddah 21921, Saudi Arabia

[3] Chemistry Department, Faculty of Applied Science, Taiz University, Taiz, Yemen

Published online: 14 July 2023

in industrial and biological testing, peroxidase enzymes are essential in a variety of industrial processes in the agricultural, analytical, environmental, and medicinal areas [6, 7]. However, the production cost is considerable due to its non-recyclability and instability, restricting its applicability. As a result, enhancing the stability of enzymes is a pressing issue that must be addressed. Enzyme immobilization is a type of enzyme engineering approach that can increase enzyme stability and has a wide range of applications [8]. Solid materials consistently immobilize enzymes for application in various production processes. Because enzymes are recyclable after immobilization, they are appropriate for use in some industrial domains in place of chemicals [9]. Owing to their remarkable biocompatibility, customizable porous topology, and high specific surface area, inorganic metal ions/clusters and coordinating organic linkers make up the new class of organic–inorganic hybrid porous materials known as metal–organic frameworks (MOFs), which have undergone significant development [10–13]. Additionally, because of the plentiful organic linkers, MOF has been widely employed to immobilize enzymes by porosity entrapment, covalent bonding precipitation, and absorption, which may preserve accessibility, activity, and the physical confinements of enzymes [14]. Enzyme immobilization by MOFs can also improve the enzyme's endurance to temperature and pH changes, resulting in a more effective water treatment strategy [15]. MOFs are attracting interest in the swiftly expanding fields of retrieval, segregation, catalysis, biomedical applications, and sensing materials because of their outstanding capabilities and the extraordinary degree of variety for both the organic and inorganic components of their structures [16]. In this project, post-synthetic method was utilized to fabricate MOF materials and then immobilized enzyme. The post-synthetic method involves modifying a MOF material with functional groups that can bind to enzymes and immobilize them within the MOF structure. In this method, the MOF material is synthesized first and then functionalized with linker molecules that have affinity for the enzyme of interest. The enzyme is then added to the functionalized MOF, where it is immobilized through binding to the linker molecules [17]. Cavka et al. [18] were the first to report a zirconium(IV)-based MOF as UiO-66. UIO-66 structure is a highly porous and stable material made up of a $Zr_6O_4(OH)_4$ octahedron cluster and 12-fold linked clusters joined by a 1,4-benzenedicarboxylate ligand. Herein, amino functionalized metal organic frameworks (NH_2-MOF-Zr) was chosen as a carrier for the immobilization of horseradish peroxidase to create an integrated enzyme system by covalent binding because of its extremely high stability and high biocompatibility. The carrier's chemical structure and morphological changes before and after enzyme immobilization were studied by different techniques. Storage stability, reusability, temperature, pH, and kinetic characteristics of immobilized enzymes were compared to soluble peroxidase.

2 Materials and methods

2-Aminoterephthalic acid (ATPA) (99%), zirconium (IV) oxychloride octahydrate ($ZrOCl_2 \cdot 8H_2O$) (99.5%), N,N-dimethylformamide (DMF) (99.8%), N-Hydroxysuccinimide (NHS) (95%), 1-Ethyl-3-(3-dimethylaminopropyl) carbodiimide (EDC) (98%), guaiacol (98%), hydrogen peroxide (H_2O_2) (35%), horseradish peroxidase (HRP) (lyophilized powder, ≥ 250 units/mg solid), phenol (97%), bisphenol A (BPA) (97%), and 4-methoxyphenol (4-MEP) (97%) were acquired from Merck (Darmstadt, Germany). All commercial chemicals were of analytical grade and utilized without any additional purification.

2.1 Fabrication of amino functionalized metal organic frameworks (NH_2-MOF-Zr)

The NH_2-MOF-Zr was fabricated according to solvothermal approach reported by Yuan et al. [19]. Generally, $ZrOCl_2$ (15 mmol) and ATPA (15 mmol) were dissolved in 80 ml DMF. Then, the reaction mixture was moved to a 100 ml Teflon liner autoclave contained 1.5 ml of concentrated hydrochloric acid. The autoclave was capped and placed in oven for 21 h at 120 °C. The obtained material (NH_2-MOF-Zr) was cooled to room temperature, then filtered, washed three times with DMF and distilled water to remove the unreacted compounds, and dried at 60 °C in drying oven.

2.2 Immobilization of HRP on NH_2-MOF-Zr

The immobilization process of HRP on NH_2-MOF-Zr was carried out as follows. Thirty milligrams of EDC was introduced to 10 ml of phosphate-buffered saline (50 mM PBS, pH 7.4) containing 300 mg NH_2-MOF-Zr and incubated for 1 h at room temperature with constant stirring. Following that, 30 mg of NHS was added to the mixture with constant stirring for 1.5 h at room temperature. The solution was then moved to a falcon tube containing 50 units of HRP in 10 ml of PBS, and immobilization was performed end-over-end for 12 h at room temperature. The product was separated through centrifugation and underwent two phosphate-buffered saline washes. The protein content was determined using the Bradford method with bovine serum albumin as the standard [20]. The immobilization yield and recovered activity were determined using the following equations:

$$\text{Immobilization Yield (IY\%)} = \frac{\text{Amount of protein introduced} - \text{Protein in the supernatant}}{\text{Amount of protein introduced}} \times 100$$

$$\text{Activity yield (AY\%)} = \frac{\text{Immobilized enzyme activity}}{\text{Iniatial activity}} \times 100$$

2.3 HRP activity assay

The horseradish peroxidase was evaluated according to Yuan and Jiang method [21] a 40 mM guaiacol, 50 mM Tris–HCl buffer pH 7.0, 8 mM H_2O_2, and the least possible amount of free enzyme or a defined weight of immobilized enzyme were supplied in a 1 ml aliquot of the reaction mixture. Once per minute, the variation in absorbance caused by guaiacol oxidation was measured. The amount of enzyme required to raise the OD to 1.0 per minute was used to define the substance's activity per unit. This experiment was performed under standard assay parameters.

2.4 Material characterization

Using an energy dispersive X-ray spectroscopy coupled scanning electron microscope (SEM, Quanta FEG 250, FEI Co., Hillsboro, USA), the morphology of the fabricated NH_2-MOF-Zr and NH_2-MOF-Zr@HRP was studied. The functional groups of NH_2-MOF-Zr and NH_2-MOF-Zr@HRP were characterized using Fourier transform infrared spectroscopy (FTIR, PerkinElmer Spectrum 100). The X-ray diffraction patterns for all samples were recorded using the XRD system (XMD-300, Unisantis, Germany), operating at a current and voltage of 30 mA and 40 kV, respectively, and over a range of $2\theta = 10–70°$ at a scan rate of 0.1°/step.

2.5 Operational stability and reusability of biocatalyst

The immobilized enzyme's operational stability is an essential parameter to consider when investigating immobilization efficiency [22]. In Tris–HCl buffer (50 mM, pH 7.0) over the course of 6 weeks at 4 °C, the operational stability of immobilized and free HRP was evaluated. The amount of enzyme leached in supernatant was evaluated via determined the enzyme activity over 6 weeks. In particular, the capability to reuse expensive enzymes and the reusability property in immobilized enzymes can be viewed as an important factor of practical applications. Reusability studies were performed on the immobilized peroxidase under the previously mentioned standard conditions. It was withdrawn out of the reaction media and then washed with 50 mM Tris-HCI buffer pH 7.2. The recovered immobilized peroxidase was then reapplied for 10 cycles. As the 100% activity control, the activity observed in the initial test was utilized to determine the proportion of activity remaining after each subsequent reuse.

2.6 Effect of PH and temperature

The pH should be taken into consideration as a significant parameter in the enzymatic reactions since the activity of enzymes is significantly impacted by environmental conditions. Using 50 mM of various pH solutions (acetate buffer pH 4–6, Tris–HCl buffer pH 6.5–9), the effect of pH on the activity of immobilized and free enzymes was assessed. To determine the impact of temperature on free HRP and NH_2-MOF-Zr@HRP, free HRP and NH_2-MOF-Zr@HRP were incubated for 15 min at various temperatures (30–80 °C) before adding substrate. The steps for determining enzyme activity were the same as in mentioned above.

2.7 Kinetic parameters

To calculate the maximum velocity (Vmax) and Michaelis–Menten constant (Km), the free HRP and NH_2-MOF-Zr@HRP activity was assessed using guaiacol and H_2O_2 as substrates at concentrations of 20–60 mM and 4–12 mM, respectively, under optimal temperatures and pH for each substrate. Using Origin/OriginPro 2018 software, the mathematical model Michaelis–Menten determined the enzyme's Km and Vmax values.

2.8 Effect of organic solvent

The effect of organic solvents on the HRP biocatalyst immobilized activity was studied in the presence of 20% (v/v) ethanol, methanol, dimethyl sulfoxide (DMSO), toluene, methanol, n-hexane, isopropanol, and butan-1-ol. The immobilized HRP was incubated in the organic solvent for 30 min before the enzyme activity determination.

2.9 Biological removal of phenols

A glass reactor soaked in a water bath at 30 °C with stirring at 100 rpm served as the reaction chamber for the enzyme-mediated operations. In the current investigation, three typical phenolic compounds—phenol, bisphenol A (BPA), and 4-methoxyphenol (4-MEP) were selected. According to Cheng et al. method [23], the initial concentrations of H_2O_2 and phenolic compounds were established at 1 mM (standard curves are shown in supplementary file; Figs. 1-3S). In the glass reactor, phenolic compounds were dissolved in 0.1 M phosphate buffer at pH 7.0, following that, H_2O_2 and enzyme were added. At regular intervals (2, 4, 6, 8 h), 1 mL of the reaction mixture was withdrawn and promptly quenched with 1 mL of methanol. By using a colorimetric approach to measure the remaining phenolic compounds, the elimination efficiency was calculated [24].

The specimen containing 200 µL of peroxidase-treated phenol was mixed with potassium ferricyanide (83.4 mM, 25 µL) and 4-aminoantipyrine (21 mM, 25 µL). After 10 min, the absorbance at 505 nm was measured.

3 Results and discussion

Recently, metal organic frameworks (MOFs) have received a great deal of admiration. Due to its unique characteristics, which include a strong connection between the MOF and enzyme, tunable porosity, thermal/chemical stability, and a high surface area for optimal enzyme loading, it has the potential to immobilize enzymes [25]. Different investigations have immobilized several enzymes onto MOFs while taking into account the aforementioned characteristics of MOF, including peroxidase [26], α-amylase [27], and lipase [28]. In this work, HRP was adopted as the model enzyme for immobilization onto amino functionalized metal organic frameworks (NH_2-MOF-Zr), then the parameters of immobilized enzyme were evaluated to assess the stability, catalytic activity, and reusability. Garcia et al. [29] developed UiO-66-NH_2 through using 2-amino-1,4-benzenedicarboxylic acid as a ligand in UiO-66. Because of its high thermal stability, large surface area, and excellent absorption capacity, UiO-66-NH_2 has received a lot of attention [30, 31]. The carrier support (NH_2-MOF-Zr) was successfully prepared by solvothermal approach as illustrated in Fig. 1. HRP immobilized by covalent binding on NH_2-MOF-Zr with immobilization yield (IY%) of 76.7% and activity yield (AY%) of 82%. In comparing these results with other results in the literature, laccase enzyme was immobilized on Fe_3O_4-NH_2@MIL-100 with the recovery activity of 70% and the immobilized yield of 61.63% [32]. HRP immobilized on CuONS–PMMA with immobilization yield of 72.8% [33]. Soybean epoxide hydrolase was successfully immobilized by Cao et al. [34] on UIO-66-NH_2, with an enzyme activity recovery of 88.0%. Table 1 shows a comparative result with other reported data. The good loading performance and efficiency of HRP were demonstrated by the immobilization of the enzyme by strongly covalent binding to NH_2-MOF-Zr, which suggested that the development of stable crosslinking by EDC/NHS between the carrier and enzymes may have been the cause of the efficiency of HRP action. As a result of the carrier's large surface area and likely excellent dispersion of the enzyme, the effectiveness of the enzyme was boosted as the steric barriers surrounding the active sites of the enzyme molecule were decreased [35, 36].

3.1 Surface morphology characterization

Using scanning electron microscopy, Fig. 2(a, b) shows a surface morphology of the obtained NH_2-MOF-Zr and NH_2-MOF-Zr@HRP. Figure 2(a) exhibits the SEM image of NH_2-MOF-Zr with particle distribution as clusters of flakes with irregular shapes. A high magnification confirms the irregular shapes of these flakes-like particles. After enzyme immobilization, a minor change occurred in morphology structure of material support (NH_2-MOF-Zr). SEM images showed a fibrous topology with a considerable number of linked tubules and an agglomerated structure (Fig. 2b). EDX (energy dispersive X-ray spectroscopy) confirmed the presence of zirconium in the chemical composition of amino functionalized metal organic frameworks (Fig. 3). The EDX has been acknowledged as a technique for bulk chemical compositions, with X-rays produced in a surface area around 2 µm in depth [37]. Figures 3, and the inset table confirmed the presence of C, N, O, S, and Zr in the structure of the synthesized NH_2-MOF-Zr@HRP and shows that 21.79% by weight of zirconium is the presence in the chemical composition of amino functionalized metal organic frameworks.

3.2 X-ray diffraction (XRD) analysis

The changed structure of NH_2-MOF-Zr before and after immobilization was investigated using the XRD. The results revealed the relatively amorphous the sample.

The formation of the hexanuclear $Zr_6O_4(OH)_4$ phase (JCPDS Card No. 01–085-9069) was evidenced by reflection peaks at $2\theta = 25.7°$; 28.44°; 43.80°; 50.62°; and 57.34° (Fig. 4), which fit well with the results reported by Pakamorė et al. [30], Chu et al. [38], and Zinatloo et al. [39]. The diffractograms show a reduction in the intensity of the NH_2-MOF-Zr peaks after immobilization, elucidating the interactions between HRP and NH_2-MOF-Zr. Our results are in agreement with that found by Chen et al. [40] and Aghajanzadeh et al. [41]. A zirconium(IV)-based MOF (UiO-66-NH_2) was prepared by Chen et al. [40] and applied for remove cationic dyes from aqueous solution. Also Aghajanzadeh et al. [41] used UiO-66-NH_2 for remove methotrexate from aqueous solution.

3.3 FTIR spectroscopy

The FTIR spectrum of NH_2-MOF-Zr and NH_2-MOF-Zr@HRP are presented in Fig. 5. Asymmetric stretching vibrations of N–H can be seen at 3424 cm^{-1}, bending frequency band of N–H at 1574 cm^{-1}, and stretching vibration of C-N at 1255 cm^{-1} [42]. The stretching vibrations of the carboxylate group correspond to the characteristic band at 1387 cm^{-1}. At 1658 cm^{-1}, an absorption peak was observed, which was attributed to C = O stretching [43]. At 1498 cm^{-1}, benzene rings' stretching vibration of the aromatic C–C ring was observed. The Zr-O stretching vibration essentially causes the peak at 660 cm^{1} to appear [31]. Furthermore, alterations in the substrate bands upon enzyme immobilization and the appearance of the glycosidic C–O–C band

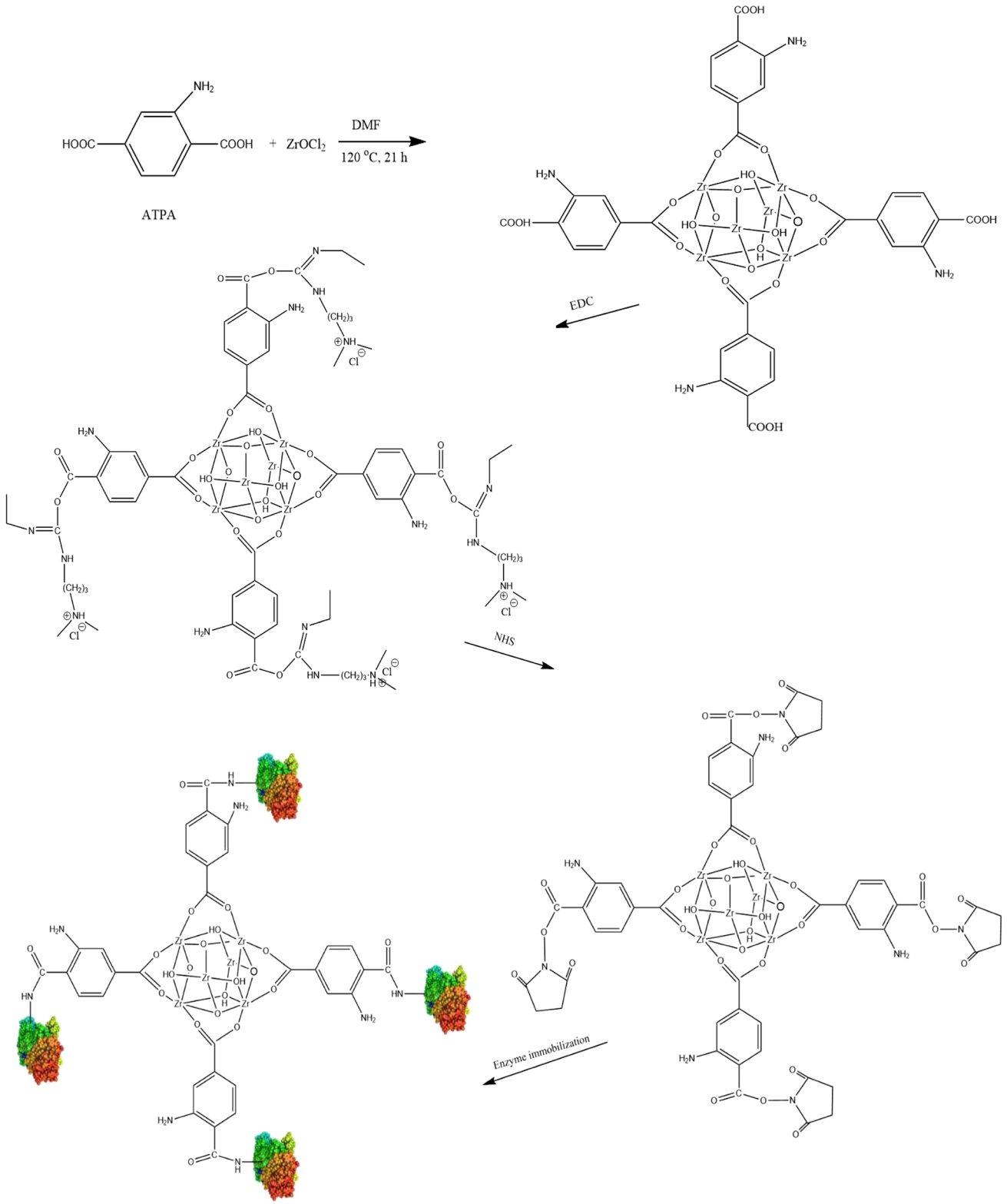

Fig. 1 Schematic representation of the fabrication of amino functionalized metal organic frameworks (NH_2-MOF-Zr) and enzyme immobilization

Table 1 Comparative results with other reported data

	[33]	[49]	[68]	[69]	This work
Immobilization yield (%)	72.8%	-	78%	66%	76.7%
Remaining activity % after 10 reuse	52%	55%	-	-	89%
Optimal pH	7.0–7.5	7.0	-	8.0	7.0–7.5
Removal efficiency of phenol% (after 5 cycle)	-	-	95%	66%	86%

at 1020 cm^{-1} could confirm to the occurrence of immobilized HRP. The bands peaks of amide I (C–O stretch) at 1628 cm^{-1}, amide II (N–H in-plane bending and C–N stretch) at 1574 cm^{-1} and 1255 cm^{-1}, and amide III (N–H and C–H deformation vibrations) at 1385 cm^{-1} were overlapped with that of 2-aminoterephthalic acid [44].

3.4 Reusability and operational stability

As compared to free enzymes, immobilized enzymes maintain their activity and can be used multiple times. The cost-effectiveness of immobilized HRP for industrial applications depends on its reusability. The oxidation of guaiacol for 10 times in succession was used to test the NH_2-MOF-Zr@HRP's reusability. After three cycles, the residual activity was 93%, after five cycles, it was 89%, and even after ten cycles, it was 59% of the initial activity, as seen in (Fig. 6a). Decreased enzymatic activity throughout the recycling cycle may be caused by high substrate concentrations and the progressive leaching of enzyme from the supporting material [45–48]. In addition, HRP activity was sustained above 50% of the initial activity up to 10 reuse cycles; hence, it can be concluded that immobilizing HRP on NH_2-MOF-Zr provides a highly stable biocatalyst. According to a report on HRP immobilized on Fe_3O_4 magnetic nanoparticles, after 10 cycles, the enzyme preserved 55% of its initial activity [49]. In another study, peroxidase was immobilized on functionalized graphene oxide and maintained 50% of its activity after nine reuses [50].

Due to free enzymes might lose their activity relatively promptly, storage stability for a prolonged period of time is one of immobilization's main advantages. By monitoring enzyme's activity each week for 6 weeks at 4 °C, the storage stability of the free enzyme and NH_2-MOF-Zr@HRP was investigated. As shown in (Fig. 6b), the maintained activity for free HRP and NH_2-MOF-Zr@HRP at the end of the third week was 82% and 91%, respectively, of the original activities. By the end of the sixth week, the residual activity for free HRP and NH_2-MOF-Zr@HRP was 31% and 74%, respectively. A slow leak observed in the HRP immobilized on NH_2-MOF-Zr. Just 3.7% of the HRP that was immobilized on NH_2-MOF-Zr leaked after 1 week. Nevertheless, during a period of 6 weeks, around 17.9% of the HRP immobilized on NH_2-MOF-Zr leaked (Fig. 6c). The enzyme's position in the NH_2-MOF-Zr channels, which provided protection for the enzyme molecules and maintained their active conformation during long-term storage, may be responsible for the improvement in storage stability [51]. Our result demonstrated that, due to the structural stabilization of HRP molecules in NH_2-MOF-Zr, the HRP immobilized on NH_2-MOF-Zr possessed greater stability than the

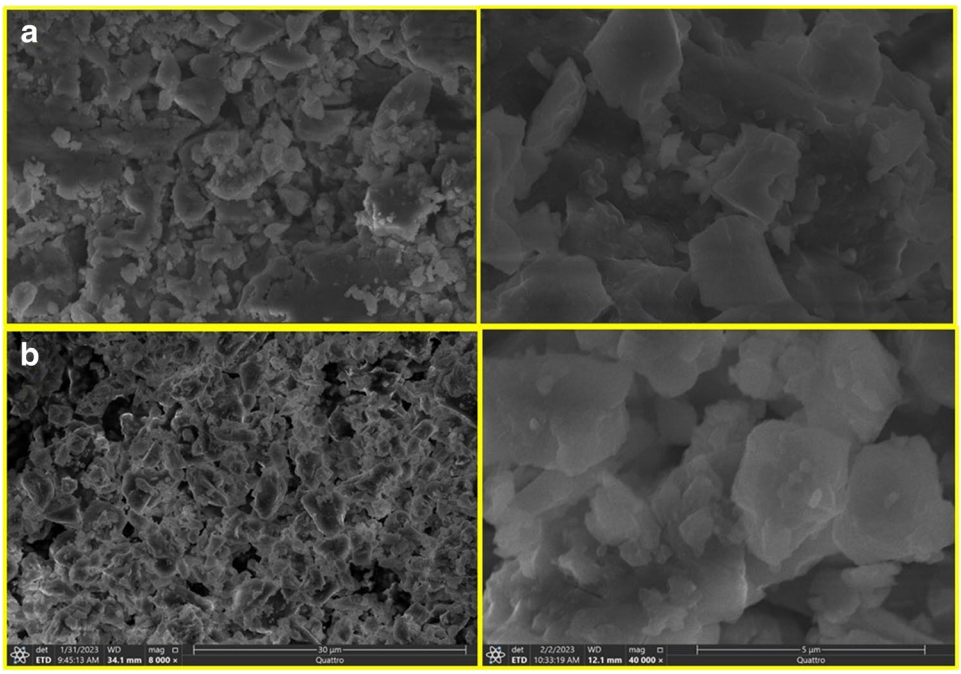

Fig. 2 Low and high magnification FESEM images of **a**) NH_2-MOF-Zr and **b**) NH_2-MOF-Zr@HRP

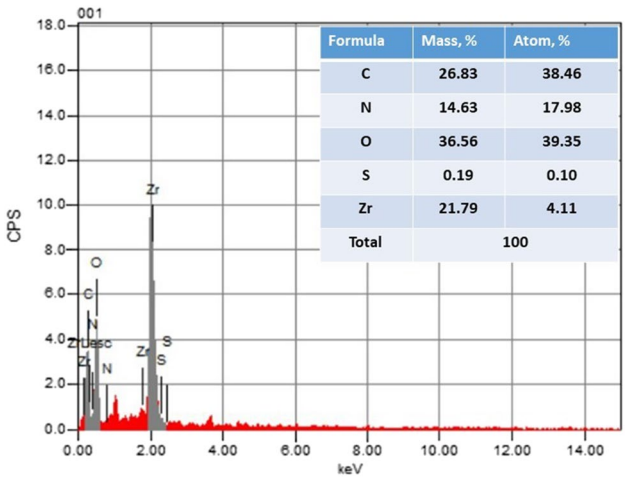

Fig. 3 The SEM–energy-dispersive X-ray (EDX) spectra of NH_2-MOF-Zr@HRP

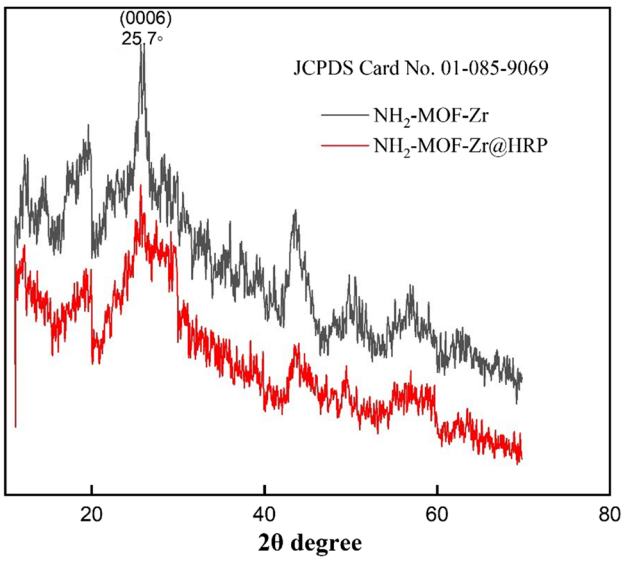

Fig. 4 The XRD patterns of (**a**) NH_2-MOF-Zr and (**b**) NH_2-MOF-Zr@HRP

free enzyme during long-term storage. On the other hand, decreased enzymatic activity throughout the recycling phase may be attributed to elevated substrate concentrations and the progressive leaching of enzyme from the supporting material [45, 52]. In a recent study, the immobilized HRP on magnetic composite microsphere preserved 71.5% of its original activity after 60 days' storage [53].

3.5 Impact of pH and temperature on the free and immobilized HRP

The impact of pH on the activity of free HRP and NH_2-MOF-Zr@HRP for oxidation of guaiacol was investigated. An important point in the applications of NH_2-MOF-Zr@HRP is the activity with varying pH. The results of the investigation on the activities of free HRP and NH_2-MOF-Zr@HRP in the pH range of (4.0–9.0) are reported in (Fig. 7a). In acetate and Tris–HCl buffers, the effects of pH on free HRP and NH_2-MOF-Zr@HRP were assessed. The studies indicate that free HRP has an optimal pH of 7.0, while NH_2-MOF-Zr@HRP has an abroad optimum pH range (7.0–7.5). At pH 9.0, the activity of NH_2-MOF-Zr@HRP was increased by twofold compared to free form. The shift in pH could be attributed to electrostatic interaction between the carrier and the enzyme. The charged carrier changes the pH at which enzymes function best once the concentration of cations near the carrier surface exceeds that of the solution [36]. Furthermore, the NH_2-MOF-Zr@HRP was significantly more robust to pH variation under acidic/basic pH conditions compared to free enzyme. The shift in the optimal pH for immobilized HRP toward a higher pH is comparable with the results reported by Mohamed et al. [54], who found that HRP immobilized on cationic maize starch had an optimal pH of 7.0. The optimal pH for immobilized HRP on Fe_3O_4Np-PMMA shifted from pH 7.0 to 7.5, according to Abdulaal et al. [55].

One of the essential aspects for the immobilization of enzymes is the enzyme activity at different temperatures. To investigate whether the optimal temperature changes after immobilization, the enzyme activities of free HRP and NH_2-MOF-Zr@HRP were evaluated at various temperatures. According to the results, the optimum activity for free HRP and NH_2-MOF-Zr@HRP was observed at 40 and 50 °C, respectively (Fig. 7b). The results were presented as a percentage of the highest activity for the enzyme at temperatures between 30 and 80 °C. In the range of 30–40 °C, the relative activity of free HRP improved with increasing temperature, whereas the relative activity of NH_2-MOF-Zr@HRP increased in the range of 30–50 °C. Furthermore, at 70 °C, NH_2-MOF-Zr@HRP maintained 67% of its activity while free HRP maintained 38%, while at 80 °C, the relative activity of free HRP was 14% and NH_2-MOF-Zr@HRP was 51%. According to the results, the material support has shielded the enzyme from undesirable alterations at high temperatures. The improvement in the optimal temperature for HRP immobilized on NH_2-MOF-Zr is compatible with results reported by Melo et al. [56], which reported that HRP immobilized on chitosan/PEG nanoparticles had an optimal temperature of 50 °C. El-Naggar et al. [57] revealed that HRP immobilized on cationic microporous starch had optimal temperature at 40 °C. Keshta et al. [58] obtained that HRP immobilized on functionalized superparamagnetic

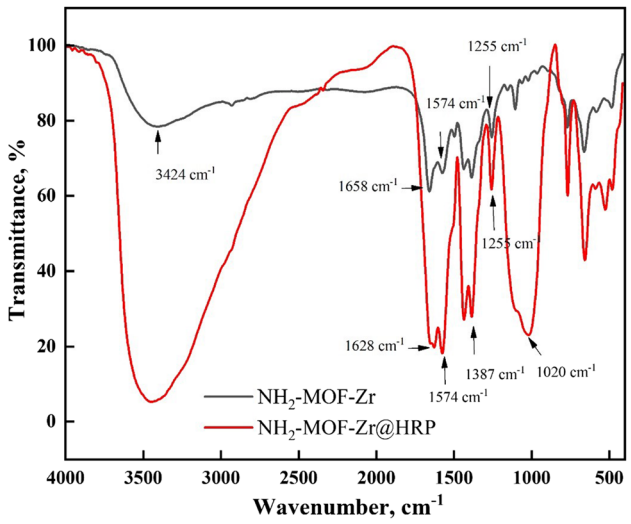

Fig. 5 FTIR spectra of NH_2-MOF-Zr and NH_2-MOF-Zr@HRP

Fe_3O_4NP performs best activity at 40 °C. Due to the interactions of HRP with the NH_2-MOF-Zr enhancing the stabilization of the HRP molecule, the immobilized HRP can preserve its active configuration even at a higher temperature, which explains why the immobilized enzyme has a higher optimal temperature than the free enzyme. It's possible that this happens because the support matrix shields the immobilized enzyme from heat and limits its mobility in response to temperature-induced denaturation, enhancing its stability over a larger temperature range. The authors [56, 59, 60] support this hypothesis.

3.6 Km and Vmax parameters

Identifying the enzyme's kinetic parameters (Km and Vmax) are essential for determining the enzyme's activity following immobilization processe. Michaelis constant (Km) reflects the substrate concentration capable of reaching half the Vmax of

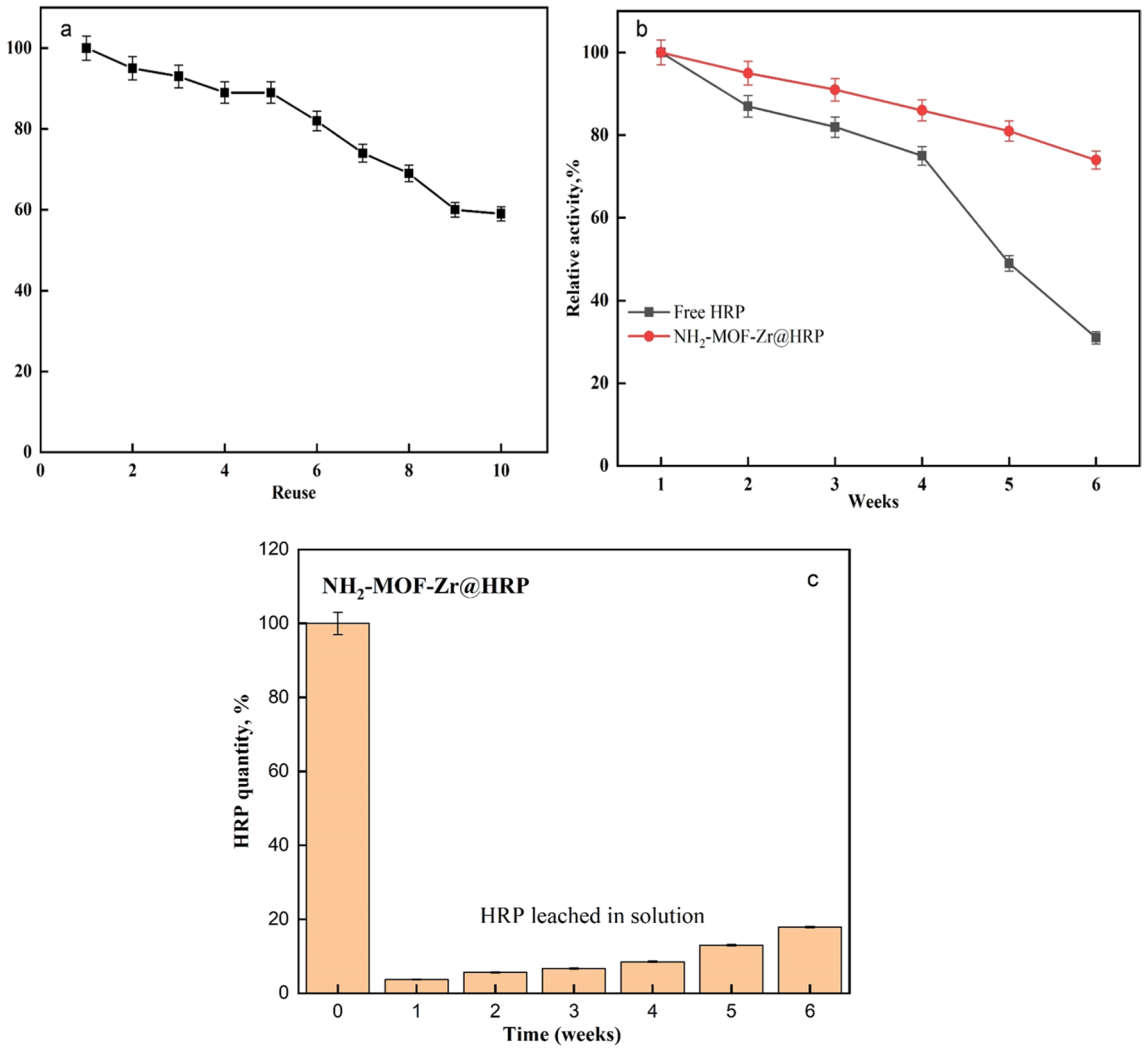

Fig. 6 **a**) Reusability and **b**) operational stability of immobilized HRP, **c**) immobilized HRP leaching in solution

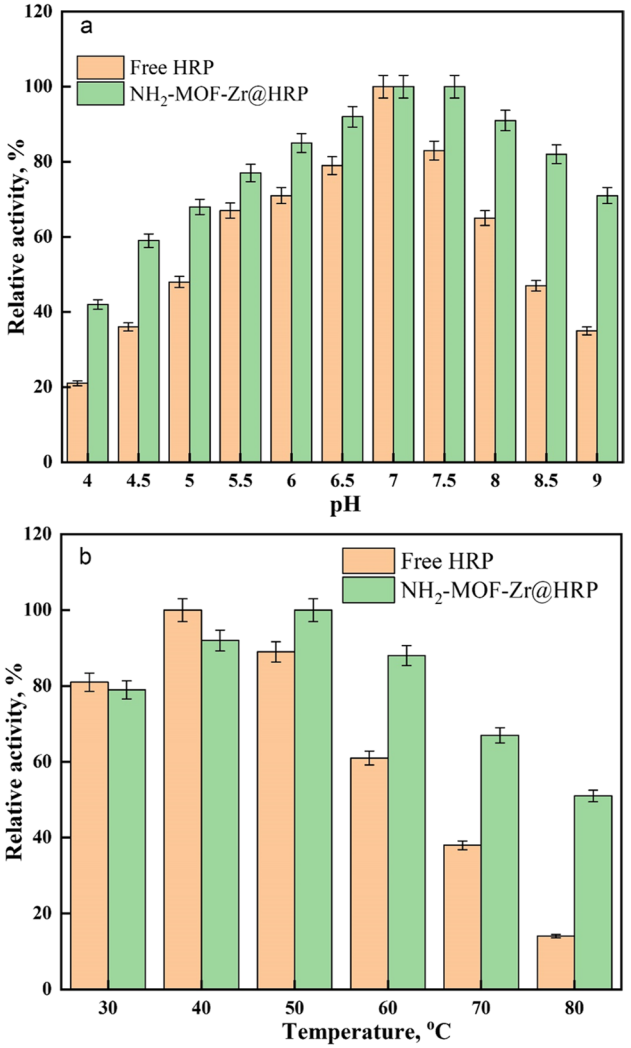

Fig. 7 Effect of **a)** PH and **b)** temperature on the activity of free and immobilized HRP

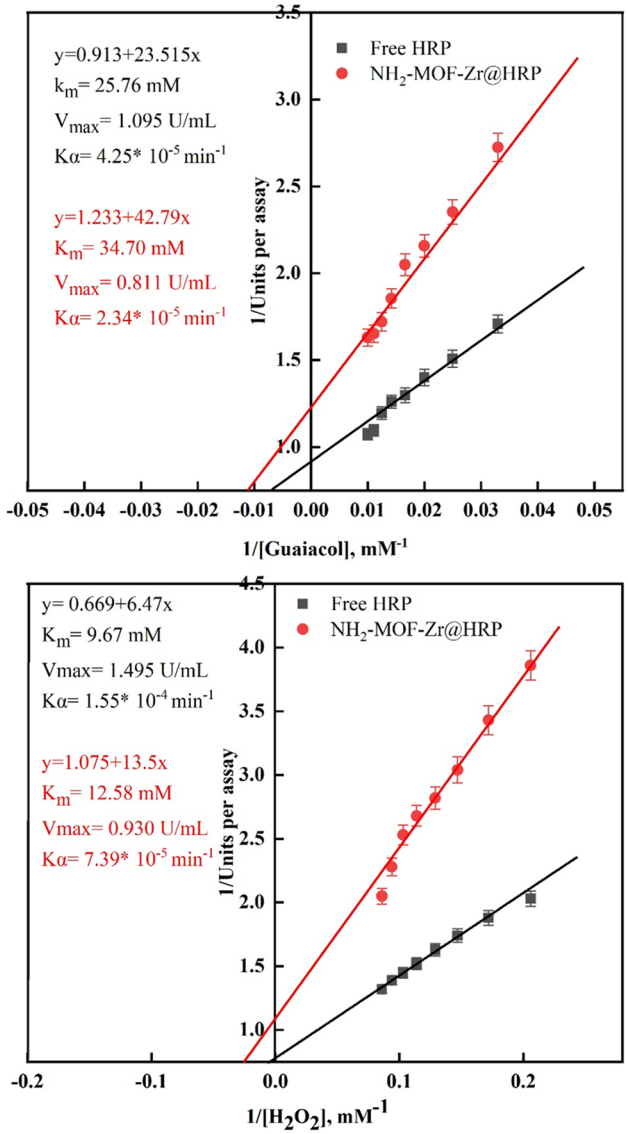

Fig. 8 Kinetic parameters of free and immobilized HRP

the reaction and indicates the degree of enzymatic adequacy for the substrate, while maximum velocity (Vmax) defines the maximum rate of an enzymatic reaction [61]. Upon enzymatic immobilization, alterations in kinetic parameters can be observed. The Vmax of the enzyme is significantly impacted by the fact that enzymatic immobilization does not guarantee that the enzyme molecules are bound in the proper configuration. Diffusion barriers are still another crucial factor in the alteration of kinetic parameters, particularly Km. An internal diffusion barrier restricts the diffusion of substrate molecules to the matrix by the presence of the enzyme within the matrix, which affects Km and Vmax. As a result, it is important to calculate the diffusion constant (Kα) from the Vmax/Km ratio [62]. Figure 8 shows estimated kinetic parameters from free HRP and NH_2-MOF-Zr@HRP. For guaiacol, the Km values of free HRP and NH_2-MOF-Zr@HRP were 25.76 and 34.70 mM and for H_2O_2 (9.67 and 12.58 Mm), respectively. On the other hand, the calculated values of Vmax of the free HRP and NH_2-MOF-Zr@HRP were 1.095 and 0.811 U/mL for guaiacol and 1.495 and 0.930 U/mL for H_2O_2, respectively. The diffusion constant (Kα) significantly decreased compared to the free HRP, indicating that the alteration in the kinetic characteristics of the enzyme may be caused by changes in the conformation of the enzyme or modifications to the microenvironment upon immobilization [63]. This phenomenon could be attributed to a restriction in the substrate's mass transfer through the reticulated networks of material support or a potential steric hindrance caused by the structural stiffness of the distorted enzyme structure after immobilization [64]. Abdulaal et al. [55] and El-Naggar et al. [57] showed an increased in km values for HRP when immobilization on PMMA incorporated with Fe_3O_4 and cationic microporous starch, respectively.

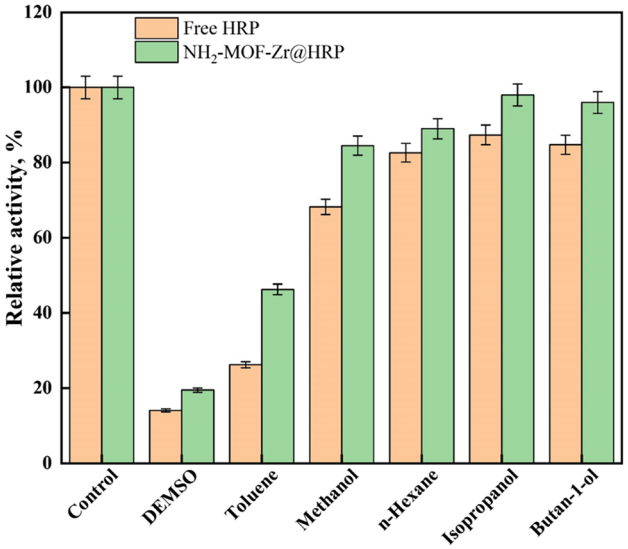

Fig. 9 Effect of organic solvent on the activity of free and immobilized HRP

3.7 Effect of organic solvent on free and immobilized HRP

Figure 9 shows the effect of organic solvents on the activity of free and NH_2-MOF-Zr@HRP; therefore, some routinely organic solvents, such as ethanol, methanol, dimethyl sulfoxide (DMSO), toluene, methanol, n-hexane, isopropanol, and butan-1-ol, were utilized in the enzyme activity assay to evaluate resistance. Free and NH_2-MOF-Zr@HRP were incubated in the presence of solvents (20%v/v) at pH 7.0 for 30 min. For free and NH_2-MOF-Zr@HRP, the highest catalytic activity was observed in isopropanol, followed by butan-1-ol and n-hexane. The free and NH_2-MOF-Zr@HRP preserved 87%, 98% of their original activity in isopropanol, 84%, 96% of their original activity in butan-1-ol, and 82%, 89% of their original activity in n-hexane. Methanol caused slightly inhibition effect on NH_2-MOF-Zr@HRP, where it preserved 84% of its original activity, while it caused moderate inhibition effect on free HRP (preserved 68% of its original activity). DEMSO and toluene caused inhibitory effect toward NH_2-MOF-Zr@HRP less than free HRP. Due to the presence of organic solvents in wastewater, it is important to investigate the stability of enzymes in such environments. Some immobilized peroxidases have reportedly shown increased resistance to organic solvents [65, 66].

3.8 Biodegradation studies of phenolic pollutants

High quantities of phenol have been found in the effluents that originate from various locations in industrial plants [67]. HRP, as a green biocatalyst, can catalyze a wide range of compounds. In this study, phenol, BPA, and 4-MEP were chosen as targets to assess enzymatic

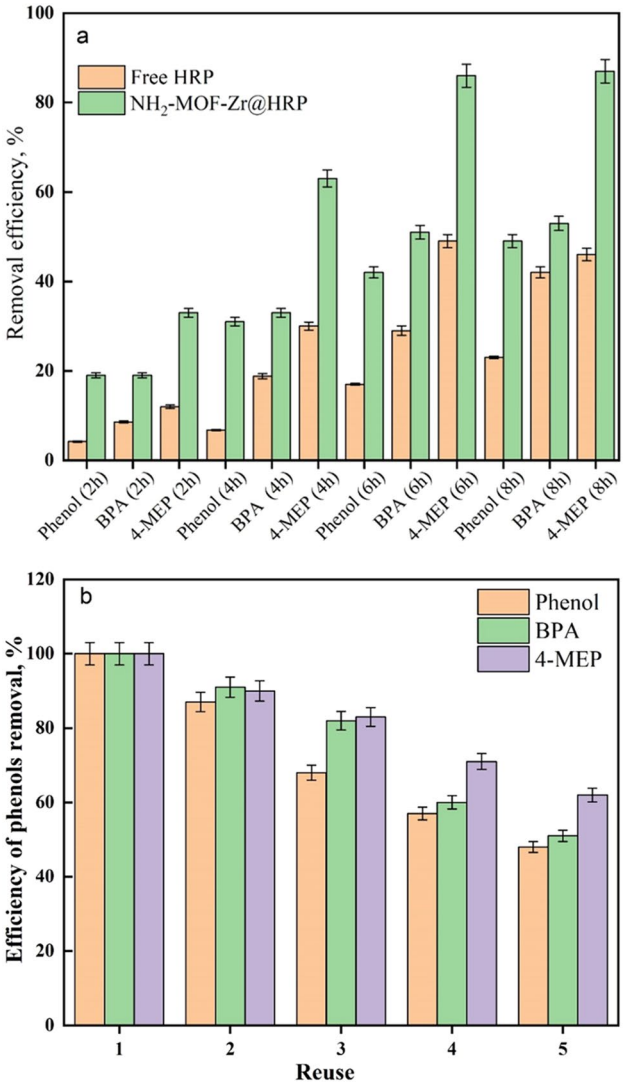

Fig. 10 **a**) Time profile for degradation of phenol, BPA, and 4-MEP by free and immobilized HRP, **b**) immobilized HRP reusability for incubation of 6 h each cycle

activity. Figure 10a illustrates the change in removal efficiency over time. About 87%, 53%, and 49% of 4-MEP, BPA, and phenol were removed by NH2-MOF-Zr@HRP during a 6-h reaction; this removal was enhanced 1.89-, 1.26-, and 2.13-folds compared that by free HRP. As can be seen in Fig. 10a, immobilization significantly improved the enzymatic performance. The study's overall results indicate that immobilization can adequately protect HRP from inactivation during the biodegradation reaction. In the recycling experiments, the biocatalytic sustainability was further evaluated. NH2-MOF-Zr@HRP were recycled after the first round of phenol, BPA, and 4-MEP removal by being withdrawn and washed and then used for the subsequent phenol, BPA, and 4-MEP removal. HRP's biocatalytic performance decreased when

reused several times, as shown in Fig. 10b. The removal efficiency of phenol, BPA, and 4-MEP after five reuse cycles was 48%, 51%, and 62%, respectively. The effect of pristine NH_2-MOF-Zr and modified NH_2-MOF-Zr by crosslinker (EDC/NHS) on the removal phenolic compounds, before enzyme immobilization, was displayed in Fig. 1S. The sharp decrease in the removal efficiency of phenols after EDC/NHS treatment can be attributed to the steric crowding and saturation of porous sites on the surface of MOFs by crosslinker EDC/NHS, which hinders the adsorption process of phenols.

4 Conclusion

In conclusion, we successfully fabricated the NH_2-MOF-Zr using a solvothermal approach and created the NH_2-MOF-Zr@HRP using EDC/NHS as cross-linker. HRP immobilized on NH_2-MOF-Zr exhibited significant catalytic activity, reusability, long-term stability, reduced leaching, and organic solvent stability, indicating better mass-transfer efficiency and enzyme accessibility, likely as a result of pore-expansion in the host material. After 10 cycles of use, the NH_2-MOF-Zr@HRP displays significant reusability, retaining up to 59% of its initial activity. The stability study revealed that after 6 weeks, NH_2-MOF-Zr@HRP was retained 74% of its initial activity. NH_2-MOF-Zr@HRP performed significantly better than free HRP enzymes in successive biodegradation studies on three phenolic compounds. During 6 h of reaction, the removal of 4-MEP, BPA, and phenol via immobilized HRP were enhanced by 1.89-, 1.26-, and 2.13-folds compared free HRP. As a result, this strategy appears to be highly useful, trustworthy, and eco-friendly, and it can be considered a technologically advantageous technique for wide use.

Supplementary Information The online version contains supplementary material available at https://doi.org/10.1007/s13399-023-04597-9.

Author contribution Y.Q.A. carried out the literature study and drafted the manuscript. Y.Q.A. and M.Z. conceived, edited, and reviewed the manuscript. All authors have read and agreed to the published version of the manuscript.

Funding The Deanship of Scientific Research (DSR) at King Abdulaziz University (KAU), Jeddah, Saudi Arabia, has funded this project under grant no (G: 342–130-1443).

Data availability Data are contained within the article.

Declarations

Ethical approval Not applicable.

Conflict of interest The authors declare no competing interests.

References

1. Khald N, Kalsoom U, Ahsan Z (2022) Bilal M (2022) Non-magnetic and magnetically responsive support materials immobilized peroxidases for biocatalytic degradation of emerging dye pollutants—a review. Int J Biol Macromol 207:387–401
2. Liu S, Huang B, Zheng G, Zhang P, Li J, Yang B, Liang L (2020) Nanocapsulation of horseradish peroxidase (HRP) enhances enzymatic performance in removing phenolic compounds. Int J Biol Macromol 150:814–822
3. Kitahara Y, Takahashi S, Tsukagoshi M, Fujii T (2010) Formation of bisphenol A by thermal degradation of poly (bisphenol A carbonate). Chemosphere 80(11):1281–1284
4. Bonefeld-Jørgensen EC, Long M, Hofmeister MV, Vinggaard AM (2007) Endocrine-disrupting potential of bisphenol A, bisphenol A dimethacrylate, 4-n-nonylphenol, and 4-n-octylphenol in vitro: new data and a brief review. Environ Health Perspect 115(Suppl 1):69–76
5. Salehi S, Abdollahi K, Panahi R, Rahmanian N, Shakeri M, Mokhtarani B (2021) Applications of biocatalysts for sustainable oxidation of phenolic pollutants: a review. Sustainability 13(15):8620
6. Keshta BE, Gemeay AH, Khamis AA (2021). Impacts of horseradish peroxidase immobilization onto functionalized superparamagnetic iron oxide nanoparticles as a biocatalyst for dye degradation. Environ Sci Pollut Res 1–13
7. Pandey VP, Awasthi M, Singh S, Tiwari S, Dwivedi UN (2017) A comprehensive review on function and application of plant peroxidases. Biochem Anal Biochem 6(1):308
8. Liang S, Wu XL, Xiong J, Zong MH, Lou WY (2020) Metal-organic frameworks as novel matrices for efficient enzyme immobilization: an update review. Coord Chem Rev 406:213149
9. Gilani SL, Najafpour GD, Moghadamnia A, Kamaruddin AH (2016) Stability of immobilized porcine pancreas lipase on mesoporous chitosan beads: a comparative study. J Mol Catal B Enzym 133:144–153
10. Li X, Liu Y, Wang J, Gascon J, Li J, Bruggen BVD (2017) Metal–organic frameworks based membranes for liquid separation. Chem Soc Rev 46:7124–7144
11. Liu J, Zhu D, Guo C, Vasileff A, Qiao S-Z (2017) Design strategies toward advanced MOF-derived electrocatalysts for energy-conversion reactions. Adv Energy Mater 7:1700518
12. Shen K, Chen X, Chen J, Li Y (2016) Development of MOF-derived carbon-based nanomaterials for efficient catalysis. ACS Catal 6:5887–5903
13. Wu M-X, Yang Y-W (2017) Metal-Organic Framework (MOF)-Based Drug/Cargo Delivery and Cancer Therapy. Adv Mater 29:1606134
14. Lian X, Fang Y, Joseph E, Wang Q, Li J, Banerjee S, Lollar C, Wang X, Zhou H-C (2017) Enzyme-MOF (metal-organic framework) composites. Chem Soc Rev 46:3386–3401
15. Han Y-H, Tian C-B, Li Q-H, Du S-W (2014) Highly chemical and thermally stable luminescent EuxTb1-x MOF materials for broad-range pH and temperature sensors. J Mater Chem C 2:8065–8070
16. Cui J, Ren S, Sun B, Jia S (2018) Optimization protocols and improved strategies for metal-organic frameworks for immobilizing enzymes: Current development and future challenges. Coord Chem Rev 370:22–41
17. Bilal M, Rashid EU, Munawar J, Iqbal HM, Cui J, Zdarta J, Jesionowski T (2023) Magnetic metal-organic frameworks immobilized enzyme-based nano-biocatalytic systems for sustainable biotechnology—A review. Int J Biol Macromol 123968
18. Cavka JH, Jakobsen S, Olsbye U, Guillou N, Lamberti C, Bordiga S, Lillerud KP (2008) A new zirconium inorganic building brick

forming metal organic frameworks with exceptional stability. J Am Chem Soc 130(42):13850–13851
19. Yuan X, Liu Y, Cao F, Zhang P, Ou J, Tang K (2020) Immobilization of lipase onto metal–organic frameworks for enantioselective hydrolysis and transesterification. AIChE J 66(9):e16292
20. Bradford MM (1976) A rapid and sensitive method for the quantitation of microgram quantities of protein utilizing the principle of protein-dye binding. Anal Biochem 72:248–254
21. Yuan ZY, Jiang TJ (2003) Horseradish peroxidase. In: Whitaker JR, Voragen A, Wong DWS (eds) Handbook of food enzymology. Marcel Dekker Inc., New York, pp 403–411
22. Almulaiky YQ, Al-Harbi SA (2019) A novel peroxidase from Arabian balsam (Commiphora gileadensis) stems: Its purification, characterization and immobilization on a carboxymethylcellulose/Fe3O4 magnetic hybrid material. Int J Biol Macromol 133:767–774
23. Cheng J, Ming S, Yu ZP (2006) Horseradish peroxidase immobilized on aluminium pillared inter-layered clay for the catalytic oxidation of phenolic wastewater. Water Res 40(2):283–290
24. Chen C, Sun W, Lv H, Li H, Wang Y, Wang P (2018) Spacer arm-facilitated tethering of laccase on magnetic polydopamine nanoparticles for efficient biocatalytic water treatment. Chem Eng J 350:949–959
25. Nadar SS, Vaidya L, Rathod VK (2020) Enzyme embedded metal organic framework (enzyme–MOF): de novo approaches for immobilization. Int J Biol Macromol 149:861–876
26. Sun H, Dan J, Liang Y, Li M, Zhuo J, Kang Y, Zhang W (2022) Dimensionality reduction boosts the peroxidase-like activity of bimetallic MOFs for enhanced multidrug-resistant bacteria eradication. Nanoscale 14(32):11693–11702
27. Atiroğlu V, Atiroğlu A, Özacar M (2021) Immobilization of α-amylase enzyme on a protein@ metal–organic framework nanocomposite: a new strategy to develop the reusability and stability of the enzyme. Food Chem 349:129127
28. Vaidya LB, Nadar SS, Rathod VK (2020) Entrapment of surfactant modified lipase within zeolitic imidazolate framework (ZIF)-8. Int J Biol Macromol 146:678–686
29. Gomes Silva C, Luz I, LlabresiXamena FX, Corma A, García H (2010) Water stable Zr–benzenedicarboxylate metal–organic frameworks as photocatalysts for hydrogen generation. Chem A Eur J 16(36):11133–11138
30. Pakamorė I, Rousseau J, Rousseau C, Monflier E, Szilágyi PÁ (2018) An ambient-temperature aqueous synthesis of zirconium-based metal–organic frameworks. Green Chem 20(23):5292–5298
31. Kurtuldu A, Eşgin H, Yetim NK, Semerci F (2022) Immobilization horseradish peroxidase onto UiO-66-NH2 for biodegradation of organic dyes. J Inorg Organomet Polym Mater 32(8):2901–2909
32. Wang D, Lou J, Yuan J, Xu J, Zhu R, Wang Q, Fan X (2021) Laccase immobilization on core-shell magnetic metal-organic framework microspheres for alkylphenol ethoxylate compound removal. J Environ Chem Eng 9(1):105000
33. Aldhahri M, Almulaiky YQ, El-Shishtawy RM, Al-Shawafi WM, Salah N, Alshahrie A, Alzahrani HA (2021) Ultra-thin 2D CuO nanosheet for HRP immobilization supported by encapsulation in a polymer matrix: characterization and dye degradation. Catal Lett 151:232–246
34. Cao SL, Yue DM, Li XH, Smith TJ, Li N, Zong MH, Lou WY (2016) Novel nano-/micro-biocatalyst: soybean epoxide hydrolase immobilized on UiO-66-NH2 MOF for efficient biosynthesis of enantiopure (R)-1, 2-octanediol in deep eutectic solvents. ACS Sustain Chem Eng 4(6):3586–3595
35. Aßmann M, Mügge C, Gaßmeyer SK, Enoki J, Hilterhaus L, Kourist R, Kara S (2017) Improvement of the process stability of arylmalonate decarboxylase by immobilization for biocatalytic profen synthesis. Front Microbiol 8:448
36. Vasicek TW, Guillermo S, Swofford DR, Durchman J, Jenkins SV (2022) β-glucosidase immobilized on magnetic nanoparticles: controlling biomolecule footprint and particle functional group density to navigate the activity–stability tradeoff. ACS Appl Bio Mater 5(11):5347–5355
37. Allehyani ES, Almulaiky YQ, Al-Harbi SA, El-Shishtawy RM (2022) In Situ coating of polydopamine-AgNPs on polyester fabrics producing antibacterial and antioxidant properties. Polymers 14(18):3794
38 Chu MN, Truong MX, Nguyen THL, Do TH, Duong TTA, Tran TKN, Pham MA (2022) Purification and characterization of high purity nano zirconia by liquid-liquid extraction using D2EHPA/p-xylenes. Inorganics 10(7):93
39. Zinatloo-Ajabshir S, Salavati-Niasari M (2016) Facile route to synthesize zirconium dioxide (ZrO2) nanostructures: structural, optical and photocatalytic studies. J Mol Liq 216:545–551
40. Chen Q, He Q, Lv M, Xu Y, Yang H, Liu X, Wei F (2015) Selective adsorption of cationic dyes by UiO-66-NH2. Appl Surf Sci 327:77–85
41. Aghajanzadeh M, Zamani M, Molavi H, Khieri Manjili H, Danafar H, Shojaei A (2018) Preparation of metal–organic frameworks UiO-66 for adsorptive removal of methotrexate from aqueous solution. J Inorg Organomet Polym Mater 28:177–186
42. Cheng J, Gu X, Liu P, Zhang H, Ma L, Su H (2017) Achieving efficient room temperature catalytic H2 evolution from formic acid through atomically controlling the chemical environment of bimetallic nanoparticles immobilized by isoreticular amine-functionalized metal-organic frameworks. Appl Catal B: Environ 218:460–469
43. Ravikumar L, Saravanan R, Saravanamani K, Karunakaran M (2009) Synthesis and characterization of new polyamides with substitutions in the pendent benzylidene rings. Des Monomers Polym 12(4):291–303
44. Almaghrabi O, Almulaiky YQ (2022). A biocatalytic system obtained via immobilization of urease onto magnetic metal/alginate nanocomposite: improving reusability and enhancing stability. Biocatal Biotransform 1–10
45. Kaushal J, Singh G (2018) Arya SK (2018) Immobilization of catalase onto chitosan and chitosan–bentonite complex: a comparative study. Biotechnol Rep 18:e00258
46. Mariño MA, Fulaz S, Tasic L (2021) Magnetic nanomaterials as biocatalyst carriers for biomass processing: immobilization strategies, reusability, and applications. Magnetochemistry 7(10):133
47. Sahu S, Shera SS, Banik RM (2019). Enhanced reusability of horseradish peroxidase immobilized onto graphene oxide/magnetic chitosan beads for cost effective cholesterol oxidase assay. The Open Biotechnol J 13(1)
48. Bilal M, Ashraf SS, Ferreira LFR, Cui J, Lou WY, Franco M, Iqbal HM (2020) Nanostructured materials as a host matrix to develop robust peroxidases-based nanobiocatalytic systems. Int J Biol Macromol 162:1906–1923
49. Mohamed SA, Al-Harbi MH, Almulaiky YQ, Ibrahim IH, El-Shishtawy RM (2017) Immobilization of horseradish peroxidase on Fe3O4 magnetic nanoparticles. Electron J Biotechnol 27:84–90
50. Rathour RK, Bhatia RK, Rana DS, Bhatt AK, Thakur N (2020) Fabrication of thermostable and reusable nanobiocatalyst for dye decolourization by immobilization of lignin peroxidase on graphene oxide functionalized MnFe2O4 superparamagnetic nanoparticles. Biores Technol 317:124020
51 Peng H, Dong W, Chen Q, Song H, Sun H, Li R, Luo H (2022) Encapsulation of nitrilase in zeolitic imidazolate framework-90 to improve its stability and reusability. Appl Biochem Biotechnol 194(8):3527–3540

52. Zucca P, Neves CM, Simões MM, Neves MDGP, Cocco G, Sanjust E (2016) Immobilized lignin peroxidase-like metalloporphyrins as reusable catalysts in oxidative bleaching of industrial dyes. Molecules 21(7):964
53. Xie X, Luo P, Han J, Chen T, Wang Y, Cai Y, Liu Q (2019) Horseradish peroxidase immobilized on the magnetic composite microspheres for high catalytic ability and operational stability. Enzyme Microb Technol 122:26–35
54. Mohamed SA, Elaraby NM, Abdel-Aty AM, Shaban E, Abu-Saied MA, Kenawy ER, El-Naggar ME (2021) Improvement of enzymatic properties and decolorization of azo dye: immobilization of horseradish peroxidase on cationic maize starch. Biocatal Agric Biotechnol 38:102208
55. Abdulaal WH, Almulaiky YQ, El-Shishtawy RM (2020) Encapsulation of HRP enzyme onto a magnetic Fe3O4 Np–PMMA film via casting with sustainable biocatalytic activity. Catalysts 10(2):181
56. Melo MN, Pereira FM, Rocha MA, Ribeiro JG, Diz FM, Monteiro WF, Fricks AT (2020) Immobilization and characterization of horseradish peroxidase into chitosan and chitosan/PEG nanoparticles: a comparative study. Process Biochem 98:160–171
57. El-Naggar ME, Abdel-Aty AM, Wassel AR, Elaraby NM, Mohamed SA (2021) Immobilization of horseradish peroxidase on cationic microporous starch: physico-bio-chemical characterization and removal of phenolic compounds. Int J Biol Macromol 181:734–742
58. Keshta BE, Gemeay AH, Khamis AA (2021) Impacts of horseradish peroxidase immobilization onto functionalized superparamagnetic iron oxide nanoparticles as a biocatalyst for dye degradation. Environ Sci Pollut Res 1–13
59. Monier M, Ayad DM, Wei Y, Sarhan AA (2010) Immobilization of horseradish peroxidase on modified chitosan beads. Int J Biol Macromol 46(3):324–330
60. Gupta N, Shrivastava A, Sharma RK (2012) Silica nanoparticles coencapsulating gadolinium oxide and horseradish peroxidase for imaging and therapeutic applications. Int J Nanomedicine 7:5491–5500
61. Liu Y, Wang M, Li J, Li Z, He P, Liu H, Li J (2005) Highly active horseradish peroxidase immobilized in 1-butyl-3-methylimidazolium tetrafluoroborate room-temperature ionic liquid based sol–gel host materials. Chem Commun 13(2005):1778–1780
62. Dwevedi A, Dwevedi A (2016) Basics of enzyme immobilization. Enzyme immobilization: advances in industry, agriculture, medicine, and the environment 21–44
63. Rani K, Chauhan N, Narang J, Jain U, Sharma S (2015) A cost effective immobilization of horseradish peroxidase nanoparticles on to easy-to-prepare activated plasticized polyvinyl-chloride vial and its application. J Nanomed Res 2(1):1–5
64. Nezhad NG, Abd Rahman RNZR, Yahaya NM, Oslan SN, Shariff FM, Leow TC (2023) Recent advances in simultaneous thermostability-activity improvement of industrial enzymes through structure modification. Int J Biol Macromol 123440
65. Wang L, Zhi W, Lian D, Wang Y, Han J, Wang Y (2019) HRP@ZIF-8/DNA hybrids: functionality integration of ZIF-8 via biomineralization and surface absorption. ACS Sustain Chem Eng 7(17):14611–14620
66. Temoçin Z, Yiğitoğlu M (2009) Studies on the activity and stability of immobilized horseradish peroxidase on poly (ethylene terephthalate) grafted acrylamide fiber. Bioprocess Biosyst Eng 32:467–474
67. Vineh MB, Saboury AA, Poostchi AA, Rashidi AM, Parivar K (2018) Stability and activity improvement of horseradish peroxidase by covalent immobilization on functionalized reduced graphene oxide and biodegradation of high phenol concentration. Int J Biol Macromol 106:1314–1322
68. Gomez JL, Bodalo A, Gomez E, Bastida J, Hidalgo AM, Gomez M (2006) Immobilization of peroxidases on glass beads: an improved alternative for phenol removal. Enzyme Microb Technol 39(5):1016–1022
69. Kim HJ, Suma Y, Lee SH, Kim JA, Kim HS (2012) Immobilization of horseradish peroxidase onto clay minerals using soil organic matter for phenol removal. J Mol Catal B Enzym 83:8–15